CATALYTIC COMBUSTION OF METHANE - THE EFFECT OF CERIUM ON PALLADIUM ALUMINA CATALYSTS

Soraia T. Brandão*, Lílian M. T. Simplício and Daniela Domingos****

brandao@ufba.br

*Universidade Federal da Bahia, PPEQ, Department of Chemical Engineering

**Universidade Federal da Bahia, Chemistry Institute

Campus de Ondina, Salvador, Bahia, Brazil, CEP. 40170-290

Abstract

PdO/Al_2O_3 and $PdO/CeO_2/Al_2O_3$ catalysts were prepared in order to investigate the role of palladium precursors and cerium addition on the catalytic properties of these systems and on the thermal stability of PdO (active phase) in the catalytic combustion of methane at high temperatures (above 600°C). The catalysts were obtained from different palladium precursors and presented distinct interactions with CeO_2/Al_2O_3, thermal stability of PdO and catalytic activity. The use of cerium improved PdO thermal stability and the cerium effect was more pronounced on the catalyst prepared from acetylacetonate indicating that a $PdO\text{-}CeO_2$ interaction is more favorable in this system.

1. Introduction

In recent decades catalytic combustion has been widely investigated as an alternative to conventional combustion due to its many practical applications both for pollution abatement and power generation. Catalytic combustion offers the possibility of producing heat and energy at much lower temperatures than conventional thermal combustion, thus reducing the emission of pollutants such as CO, NOx and unburned hydrocarbons (UHC) [1-9].

Noble metals display considerable activity in hydrocarbon oxidation and palladium has been widely reported in literature [2 - 5, 7, 8, 10, 11 and 12] as the catalyst of choice in methane combustion. Some of the reasons for this include: first, palladium-based catalysts are extremely active in methane oxidation which guarantees ignition at low temperatures, below 400°C; second, palladium species formed under reaction conditions (up to 800°C) present low volatility; finally, these systems have the unique capability of temperature self-control associated with the reversible PdO (active) /PdO(inactive) transformation.

Catalytic combustion at high temperatures (over 600°C) requires thermally stable catalysts, resistant not only to support sintering but also resistant to decomposition and/or sintering of the active phase. There is general agreement in the literature [1-12] that the active phase of palladium catalysts is palladium oxide, PdO. This, in turn, is only thermodynamically stable at temperatures below 600°C. Above 600°C PdO decomposes into metallic palladium which is thermodynamically stable in the high temperature range. As metallic palladium is much less active than palladium oxide in methane combustion, this decomposition implies a loss of catalytic activity.

The use of rare earth oxides has been described in literature [9, 11-16] as one of the best alternatives for stabilization of the support and the active phase. According to these studies, while La_2O_3 is an excellent stabilizer of the specific area of supports such as Al_2O_3 and ZrO_2,

CeO_2 is an excellent alternative to stabilize PdO since it hinders PdO reduction and promotes Pd re-oxidation when PdO-CeOx contact is favorable.

In this work the characterization and reactivity of cerium-alumina-supported Pd catalysts in the catalytic combustion of methane are investigated. In particular, the effect of a palladium precursor on reactivity and PdO thermal stability of Pd-supported catalysts is considered. In order to better understand the CeO_2 effect PdO/Al_2O_3 and $PdO/CeO_2/Al_2O_3$ samples were prepared from different Pd precursors (chloride, nitrate, acetylacetonate). The samples were characterized by means of different techniques (see section 2) and tested in the combustion of methane.

2. Methodology

Preparation of the Catalysts

The alumina Pural SB (BET surface area of 193 m^2g^{-1}) used as support was supplied by Condea. This support was calcined at 600°C for 10 h before use. High purity palladium reagents, $Pd(NO_3)_2$, $Pd(C_5H_7OO)_2$ and $PdCl_2$, supplied by Merck, were used as precursors.

PdO/Al_2O_3 catalysts with nominal Pd loading near 3% w/w were prepared from alumina impregnation with solutions of $Pd(NO_3)_2$, $Pd(C_5H_7OO)_2$ and $PdCl_2$. The samples prepared from palladium chloride and nitrate were obtained by alumina impregnation with aqueous solutions of these salts. The sample prepared from palladium acetylacetonate was obtained by alumina wetness impregnation with a toluene solution of this precursor. After impregnation the materials were dried at 110°C for 12 hours and calcined at 1000°C for 5 hours under air flow (50 $mL.min^{-1}$). The samples obtained from palladium chloride, nitrate and acetylacetonate were labeled PAC, PAN and PAA, respectively.

$PdO/CeO_2/Al_2O_3$ catalysts with nominal Pd loading near 3% w/w were prepared from CeO_2/Al_2O_3 impregnation with solutions of those precursors. CeO_2/Al_2O_3 support was obtained by alumina impregnation with aqueous solution of $Ce(NO_3)_3$, followed by drying at 110°C and calcination at 1000°C for 5 hours. After CeO_2/Al_2O_3 impregnation with the solutions of palladium precursors mentioned above, the materials were dried at 110°C for 12 hours and calcined at 1000°C for 5 hours under air flow. The samples were labeled PAC-Ce, PAN-Ce and PAA-Ce. Table 1 shows the chemical analysis data for all the prepared catalysts.

Table 1: Chemical Analysis Data

Sample	Pd (%)	CeO_2 (%)
PAC-1	3.0	-
PAN-1	2.8	-
PAA-1	2.7	-
PAC-Ce	2.5	10.1
PAN-Ce	2.8	10.1
PAA-Ce	2.6	10.1
CeO_2/Al_2O_3	-	10.1

Characterization

The X-ray diffraction measurements were carried out on a Shimadzu apparatus (XRD-6000). The Cu Kα radiation (λ = 1.5418 Å) and the following experimental conditions were used: 2θ range = 10-80°, step size = 0.02° and time per step = 4.80 s. The powder samples were analyzed without further treatment.

The palladium and cerium content on the samples were obtained by X-ray fluorescence on a Shimadzu WDS apparatus (XRF-1800).

Specific area measurements were carried out through N_2 adsorption on an ASAP 2000 using the BET method.

PdO thermal stability was studied using Temperature Programmed Oxidation (TPO) in a flow system. 100 mg of the catalyst was loaded into a quartz reactor and heated in a 5% O_2/He flow (30 mL.min-1) at a rate of 5°C.min-1 from room temperature to 1000°C. The samples were cooled to room temperature under the same O_2/He flow. Oxygen in the reactor outlet was detected by using a quadrupole mass spectrometer, Balzers QMS-200. The mass-to-charge ratio (m/e) = 32 was used to monitor the oxygen concentration.

TEM measurements were carried out with a JEOL 100CXII operating at 100 kV. The powder was ultrasonically dispersed in ethanol and the suspension was deposited on a copper grid coated with a porous carbon film.

XPS experiments were recorded on a Vacuum generators Escalab VG MK1 spectrometer operating at constant pass energy (50 eV) with an unmonochromated Mg Kα source (200 W) under 10-8 mbar. After the pretreatments, the samples were placed in an inert gas atmosphere and rapidly transferred into the spectrometer. The binding energy was referenced to the C 1s binding energy of 285.0 eV.

Temperature Programmed Catalytic Activity Tests

Transient flow microreactor experiments were performed in a quartz tubular fixed bed microreactor loaded with 100 mg of catalyst diluted with 100 mg of quartz granules. The reactor was inserted into an electric furnace driven by a proportional-integral-derivative temperature controller/programmer. The temperature of the catalyst was measured and controlled by means of a K-type thermocouple sliding in a quartz compartment beside the catalyst bed. The samples were heated to 1000°C at a rate of 10°C.min-1, under a flow of 100 mL.min-1 of a mixture 0.5% CH_4, 2% O_2 and 97.5% N_2. The reactant gases were fed into the reactor by means of an electronic mass flow meter controller MKS 247 and the reactor operated at GHSV = 60,000 mL.gcat-1.h-1. The effluent gases were detected by using a quadrupole mass spectrometer, Balzers QMS-200, connected at the reactor outlet. The following mass-to-charge ratios (m/e) were used to monitor the concentrations of products and reactants: 15 and 16 (CH_4), 18 (H_2O), 28 (CO), 32 (O_2), 44 (CO_2).

3. Results and Discussion

The identification of the palladium phases in the catalysts was carried out by X-ray diffraction. The XRD patterns of the catalysts are shown in Figure 1. The catalysts without CeO_2 revealed the presence of characteristic peaks of γ-Al_2O_3 and δ-Al_2O_3. Regarding

palladium, the predominant phase in these samples is the tetragonal form of PdO (peaks at 2θ = 34°, 42°, 55° and 61°). Cubic metallic palladium was also detected (peaks at 2θ = 39.9°, 46.4° and 67.8°). The XRD patterns of the cerium containing samples indicate the presence of γ-Al_2O_3, δ-Al_2O_3, Pd and PdO phases, characterized by the peaks at 2θ values previously mentioned. The CeO_2 phase, in a hexagonal fluorite structure, was also identified. Characteristic peaks of this phase can be observed at 2θ = 28.5°, 33.1°, 47.5°, 56.3°, among others.

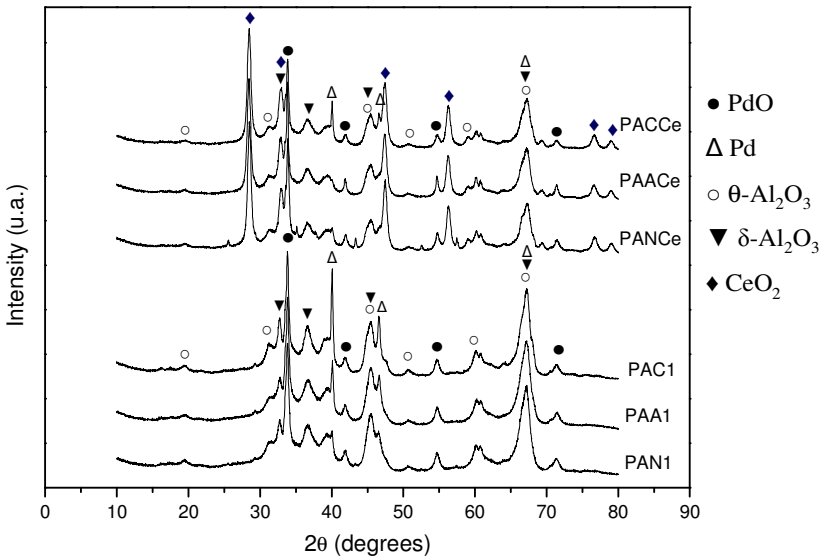

Figure 1. XRD patterns of the support and the catalysts calcined at 1000°C

The thermal stability of PdO was studied by Temperature Programmed Oxidation (TPO). The TPO profiles of the samples were similar, exhibiting reduction peaks between 780 and 840ºC during the heating ramp (Figure 2). PdO is thermodynamically unstable in this temperature range so these peaks are attributed to the decomposition of palladium oxide into metallic palladium [18]. For each sample TPO profiles illustrated the presence of two oxygen peaks which indicates that during heating the PdO decomposition in these samples would occur in two distinct steps. The literature [2, 7] presents similar results and suggests that these decomposition steps were related to different PdO crystallites: PdO in contact with residual metallic palladium (1st peak) and PdO in contact only with other PdO crystallites (2nd peak).

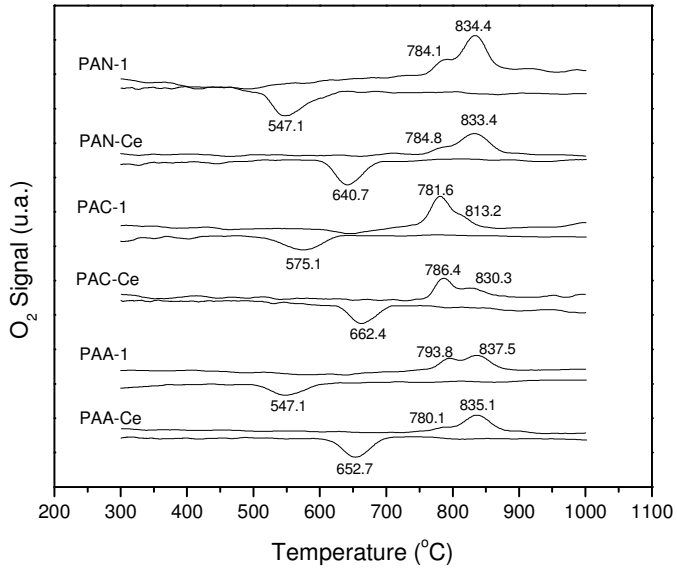

Figure 2. TPO profiles of the catalysts calcined at 1000°C.

The TPO profiles also reveal a peak that reflects oxygen consumption between 540 and 580ºC during the cooling ramp. This peak is attributed to the re-oxidation of Pd, regenerating PdO. The results also showed that Pd re-oxidation begins at lower temperatures than the onset temperature of PdO decomposition. According to the literature [2, 7, 19-23], complete oxidation of the metal to the oxide is known to be a slow process which explains the hysteresis observed in this process.

Table 2 shows PdO decomposition and re-oxidation temperatures for each sample. The results indicate that re-oxidation occurs at higher temperatures for the samples modified with cerium demonstrating the stabilizing effect of cerium. According to the literature [2, 14, 17, 24, 25] the cerium effect consists of improving palladium oxide thermal stability when the PdO-CeOx interaction is favorable. In agreement with previous data [14], this effect is directly related to the ability of cerium to undergo the $(Ce^{3+})/(Ce^{4+})$ transformation (equation 1).

$$CeO_2 \rightleftharpoons CeO_{2-X} + 0.5\ XO_2 \qquad (1)$$

Table 2. PdO decomposition and Pd reoxidation temperatures.

Catalyst	Td_1 (°C)	Td_2 (°C)	Tr (°C)	$Td_2 - Tr$ (°C)	$\Delta Td_2 - Tr$ (°C)
PAN-1	784.1	834.4	547.1	287.3	
PAN-Ce	784.8	833.4	640.7	192.7	94.6
PAC-1	781.6	813.2	575.1	238.1	
PAC-Ce	786.4	830.3	662.4	167.9	70.2
PAA-1	793.8	837.5	547.1	290.4	
PAA-Ce	780.1	835.1	652.7	182.4	108

Td = decomposition temperature e Tr = reoxidation temperature

In addition to the high mobility of oxygen species this ability makes cerium an excellent PdO stabilizer, supplying the oxygen necessary to maintain Pd as an oxide when the PdO-CeOx contact is favorable.
In order to investigate which system is more favorable for this PdO-CeO_2 interaction, TPO profiles of PdO/CeO_2/Al_2O_3 and PdO/ Al_2O_3 samples were compared (Figure 2). The TPO profiles also indicate that (i) presence of CeO_2 shifted palladium oxidation to higher temperatures improving PdO thermal stability, (ii) The cerium effect on PdO thermal stability is strongly dependent on the nature of the palladium precursor.

The effect of CeO_2 on PdO thermal stability for each precursor can be viewed in Table 2. The column Td_2 - Tr reflects the temperature range in which palladium is in the metallic phase. The results showed that the addition of cerium shifted palladium re-oxidation to higher temperatures decreasing this temperature range, which increases PdO thermal stability.

The column ΔTd_2 – Tr, reflects the temperature range in which palladium is in the metallic phase. It shows significant differences between the cerium-containing and cerium-free catalysts. Greater differences indicate a better stabilizing cerium effect. In addition, the effect

of improving PdO thermal stability is more pronounced in the sample prepared using acetylacetonate as a precursor, which indicates that PdO-CeO_2 interaction is more favorable in this sample.

These results confirm that the ability of cerium to improve PdO thermal stability is directly related to the nature of the palladium precursor and are in agreement with the literature [17] which indicates that the use of different palladium precursors in the presence of cerium affects Pd-Ce interaction and Pd dispersion in the catalysts. In particular, the results obtained in these studies showed that acetylacetonate promotes a strong Pd-Ce interaction which favors the re-dispersion of Pd crystallites in a more organized bi-dimensional structure.

TEM analysis was carried out in order to investigate PdO and CeO_2 distribution over alumina surface and the results obtained can be seen in Figures 3 and 4. For the PdO/Al_2O_3 catalysts, TEM images showed the presence of large PdO particles on the alumina surface which is related to the high calcination temperature of these samples.

TEM results obtained with CeO_2 modified samples revealed the presence of CeO_2 well-dispersed particles and large PdO particles. These images suggest that PdO is in contact with CeO_2 and covering these particles. These results are supported by the preparation method in which PdO was impregnated on the CeO_2-Al_2O_3 support.

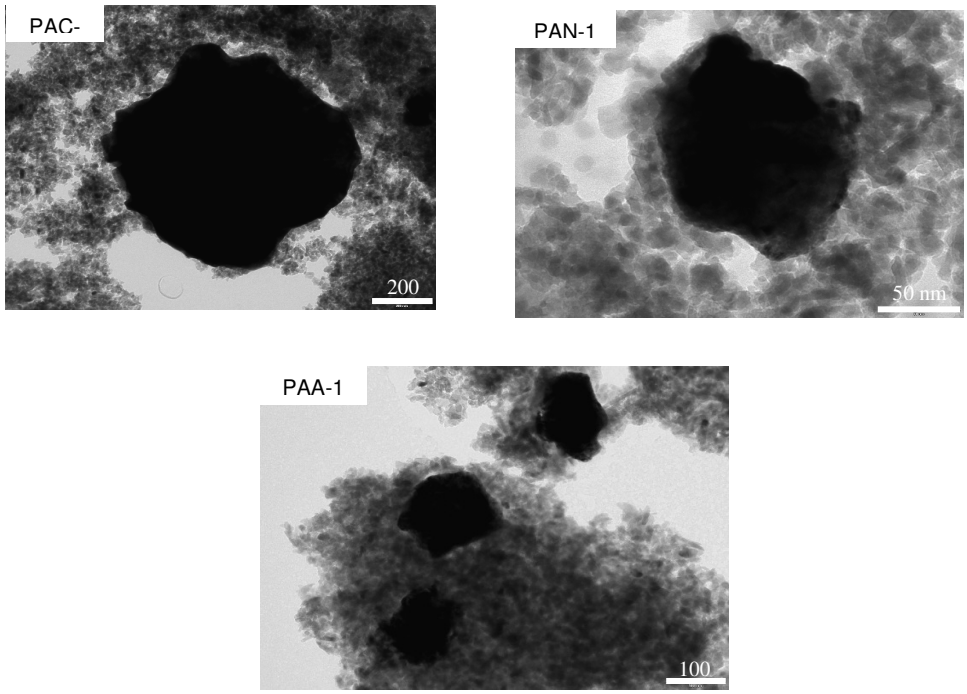

Figure 3. TEM images of the catalysts PAC-1, PAA-1 and PAN-1.

XPS results are shown in Table 3 and indicate a binding energy for Pd3d5/2 from 336.50 and 337.10 eV. Similar results have been reported in the literature for Pd^{2+} in PdO (25-28). According to Voogt et al. [25, 26] the binding energy for Pd^{+2} in PdO is 336.4±0.1 and these higher values are typically obtained in fully oxidized samples, directly after oxidation, These higher binding energies are therefore probably due to an excess of oxygen.

Table 3.: Binding energy values for $Pd3d_{5/2}$ for the catalysts calcined at 1000°C

Catalyst	B.E.Pd_{3d} (eV)
PAC-1	336.50
PAN-1	336.90
PAA-1	336.50
PAC-Ce	336.70
PAN-Ce	336.60
PAA-Ce	337.10

Table 3 also shows the calculated Pd/Al and Ce/Al ratios on the catalyst bulk and surface. The results indicate that, for the samples without cerium, the catalysts with smaller PdO particles present a higher Pd/Al ratio on the surface than in the bulk. This can be explained by the fact that in smaller particles the internal layers are more accessible to radiation than in the larger ones.

For the samples prepared with cerium, the surface Ce/Al ratio was smaller than the bulk one. This indicates that CeO_2 is not completely accessible to the radiation, which suggests that PdO is covering some CeO_2 particles. This is in agreement with TEM results (Figure 4) which shows that PdO is over the CeO_2 well dispersed particles.

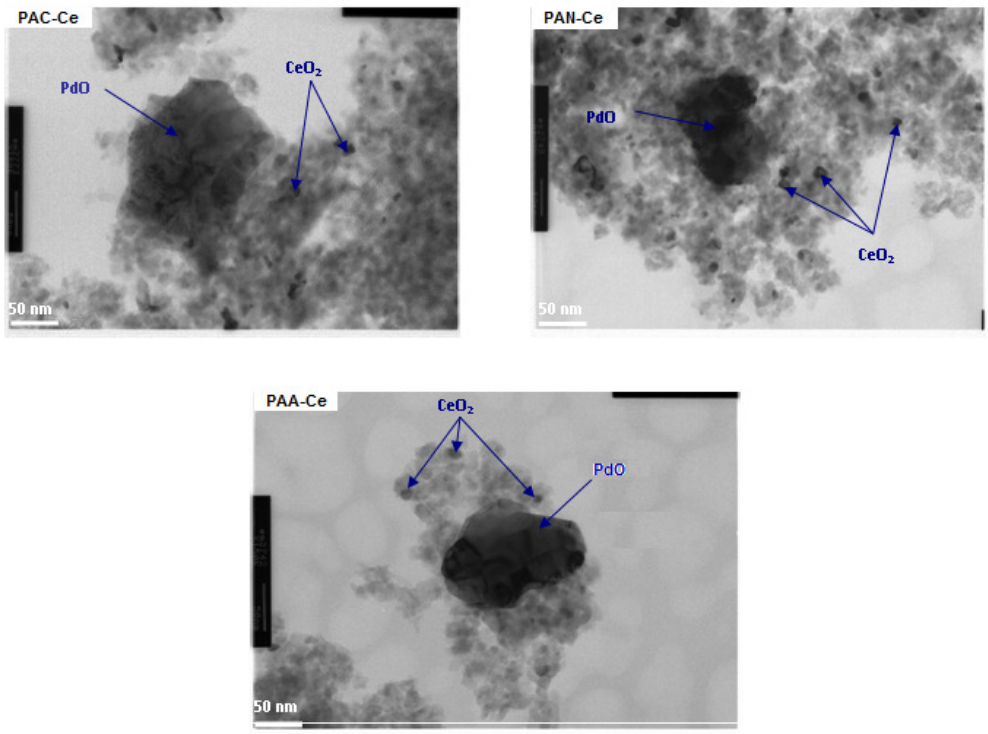

Figure 4. TEM images of the catalysts PAC-Ce, PAA-Ce and PAN-Ce

The TPSR profiles for the samples without CeO_2 are shown in Figures 5, 6 and 7. These results indicate that all catalysts presented excellent conversion of methane in a wide temperature range. They presented an ignition temperature of between 300 and 400°C and reached maximum conversion (above 95%) between 650 and 710°C. The results also indicate

that the precursor did not have a great influence on the catalytic behavior of these systems. This behavior can be attributed to the fact that the PdO particle size of these catalysts is similar, which leads to similar methane conversion values and/or ignition temperatures.

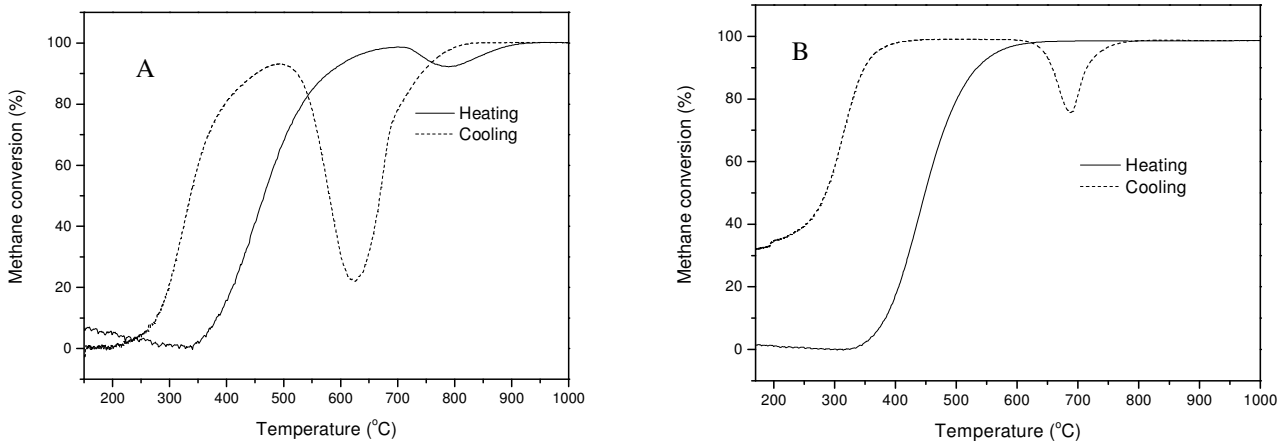

Figure 5. Methane conversion curve obtained with PAA-1 (A) and PAA-Ce (B) catalysts.

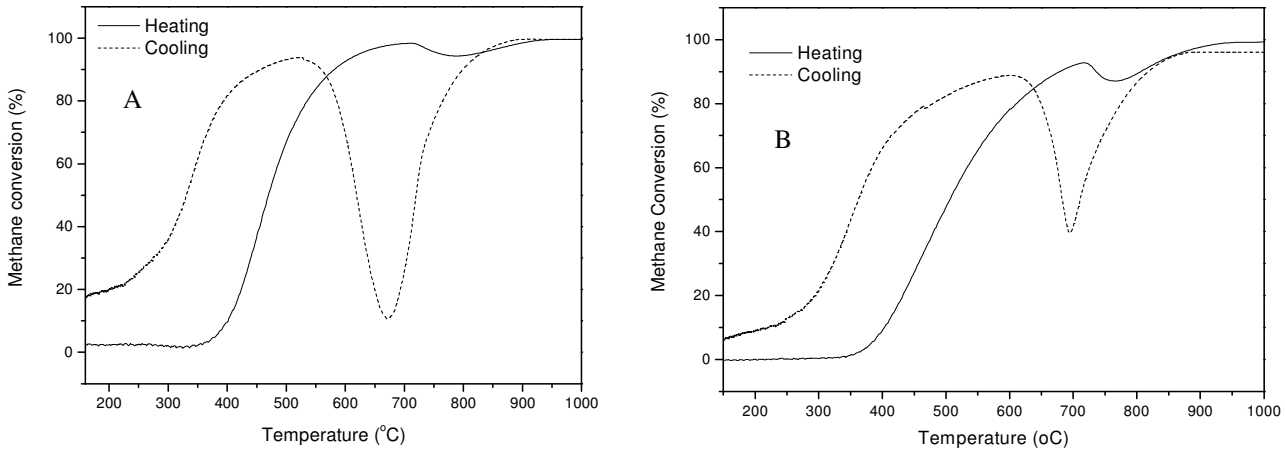

Figure 6. Methane conversion curve obtained with PAC-1 (A) and PAC-Ce (B) catalysts

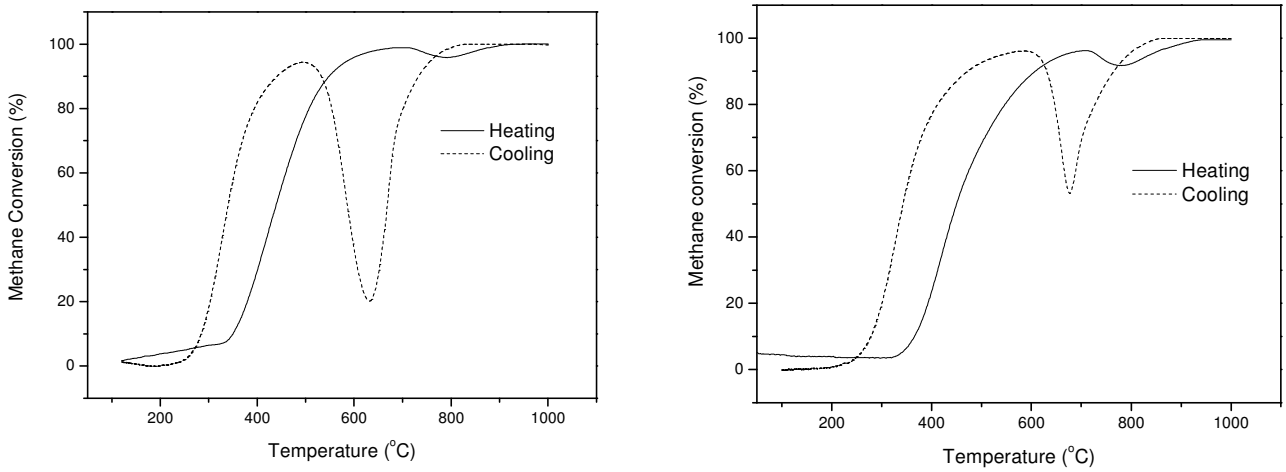

Figure 7. Methane conversion curve obtained with PAN-1 (A) and PAN-Ce (B) catalysts.

Using ignition temperature as a measure of catalytic activity for these systems, we observe that the catalyst PAN-1 presents the lowest ignition temperature. The sequence observed for

the activity is PAN-1 ≥ PAA-1 > PAC-1 (Table 4).The cerium effect on PdO thermal stability is also illustrated by the loss of activity during the TPSR cooling ramp. The profiles for all catalysts indicate that during the cooling ramp the catalytic activity decreases, reaches a minimum and is then regenerated due to Pd re-oxidation. PdO thermal stability is directly related to this loss/regeneration of activity. With more stable PdO particles palladium re-oxidation and activity regeneration during the cooling ramp is more favorable.

Table 4. Ignition temperature obtained with the catalysts calcined at 1000°C.

Catalyst	T_{10} (°C)
PAN1	326
PAN-Ce	305
PAC1	350
PAC-Ce	345
PAA1	333
PAA-Ce	338

The results obtained are consistent with TPO results and indicate that the loss of activity during the cooling ramp is less pronounced on cerium modified samples, suggesting a higher stability of PdO particles. The TPSR profiles also show that the cerium effect is more pronounced on the catalyst prepared from acetylacetonate, which indicates that the PdO-CeO_2 interaction is more favorable in this system.

4. Conclusions

The results obtained with cerium modified catalysts show that different palladium precursors show distinct interactions with the CeO_2/Al_2O_3 system. As a result, several properties, such as PdO thermal stability and catalytic behavior, are affected. The use of cerium improved PdO thermal stability and this was more pronounced on the catalysts prepared using acetylacetonate as a precursor.

5. Acknowledgements

This work was supported by CNPq and by Petrobras. The XPS measurement were performed by Prof. Maria das Graças Rocha and Dr. Pascal Bargiela and TEM experiments were carried out by Ms Patricia Beaunier (LRS, University Pierre et Marie Curie) and M. Frederic Herbst (ITODYS, University Paris-Diderot) to whom we are most grateful.

6. Nomenclature

PAC = Catalyst with PdO from chloride precursor.
PAN = Catalyst with PdO from nitrate precursor.
PAA = Catalyst with PdO from acetylacetonate.
PAC-Ce = PdO - Ce catalyst
λ = Cu Kα radiation
XRD = X-ray diffraction
2θ= Diffraction angle

6. References

[1] J. H. Lee, D. L. Trimm, Fuel Process Technol. 42 (1995) 339-359.
[2] G. Groppi, C. Cristiani, L. Lietti, C. Ramella, M. Valentini, P. Forzatti, Catal. Today 50 (1999) 399-412.
[3] J. W. Geus, J. C. Van Giezen, Catal. Today 47 (1999) 169-180.
[4] G. Centi, J. Mol. Catal. A-Chem. 173 (2001) 287-312.
[5] T.V. Choudhary, S. Banerjee, V.R. Choudhary, Appl. Catal. A-Gen. 234 (2002) 1-23.
[6] P. Gélin, M. Primet, Appl. Catal. B-Environ. 39 (2002) 1-37.
[7] P. Forzatti, Catal. Today 83 (2003) 3-18.
[8] P. Gélin, L. Urfels, M. Primet, E. Tena, Catal. Today 83 (2003) 45-57.
[9] A. K. Neyestanaki, F. Klingstedt, T. Salmi, D. Y. Murzin, Fuel 83 (2004) 395-408.
[10] D. Ciuparu, M. R. Lyubovsky, E. Altman, L. D. Pfefferle, A. Datye, Catal. Rev. 44 (2002) 593-649.
[11] Y. Deng, T. G. Nevell, Catal. Today 47 (1999) 279-286.
[12] L. M. T. Simplício, S. T. Brandao, E. A. Sales, L. Lietti, F. Bozon-Verduraz, Appl. Catal. B-Environ. 63 9-14 (2006).
[13] P. Euzen, J. H. Le Gal; B. Rebours, G. Martin, Catal. Today 47: 19-27 (1999).
[14] S. Colussi, C. Leitenburg, G. Dolcetti; A. Trovarelli, J. Alloy. Compd. 374 387-392 (2004).
[15] M. A. Fraga, E. S. Souza, F. Villain, L. G. Appel, Appl. Catal. A-Gen. 259: 57-63 (2004).
[16] Y. Ozawa, Y. Tochihara, A. Watanabe, M. Nagai, S. Omi, Appl. Catal. A-Gen. 258: 261-267 (2004).
[17] R. S. Monteiro, L. C. Dieguez, M. Schmal, Catal. Today 65: 77-89 (2001).
[18] K. Sekizawa, H. Widjaja, S. Maeda, Y. Ozawa, K. Eguchi, Appl. Catal. A-Gen. 200: 211-217(2000).
[19] P. O. Thevenin, A. Alcalde, L. J. Pettersson, S. G. Järås, J. L. G. Fierro, J. Catal. 215: 78-86 (2003).
[20] R.J. Farrauto, M.C. Hobson, T. Kennelly, E. M. Waterman, Appl. Catal. A-Gen. 81 227-237(1992).
[21] J. G. McCarty, Catal. Today 26: 283-293 (1995).
[22] P. Forzatti, G. Groppi, Catal. Today 54: 165-180 (1999).
[23] A. K. Datye, J. Bravoa, T. R. Nelson, P. Atanasova, M. Lyubovsky, L. Pfefferle, Appl. Catal. A-Gen. 198:179-196 (2000).
[24] A. L. Guimaraes, L. C. Dieguez, M. Schmal, J. Phys. Chem. B 107 (2003) 4311-4319.
[25] E. H. Voogt, A. J. M. Mens, O. L. J. Gijzeman, J. W. Geus, Surf. Sci. 350: 21-31(1996).
[26] E. H. Voogt, A. J. M. Mens, O. L. J. Gijzeman, J. W. Geus, Catal. Today 47: 321-323(1999).
[27] M. Brun, A. Berthet, J. C. Bertolini, J. Electron. Spectrosc. 104: 55-60 (1999).
[28] S. Suhonen, M. Valden, M. Pessa, A. Savimaki, M. Harkonen, M. Hietikko, J. Pursiainen, R. Laitinen, Appl. Catal. 207: 113-120 (2001).